

# Scalable Synchrophasors Communication Network Design and Implementation for Real-Time Distributed Generation Grid

Hamid Gharavi, *Life Fellow, IEEE*, and Bin Hu, *Senior Member, IEEE*

**Abstract**—There has been a growing interest in the deployment of phasor measurement units (PMUs) not only in high-voltage transmission, but in lower-voltage distribution systems. For a distributed generation (DG) grid, this would require deployment of PMUs at critical locations, which implies accurate phase measurement with the support of a low delay, highly reliable network infrastructure. In the absence of such a network, the most cost-effective solution would be to consider a wireless network to support centralized control for situational awareness in the transmission, as well as the DG grid environment. Therefore, the main objective in this paper is to design and implement a scalable synchrophasor network using wireless LAN technology to assess network performance and requirements under real-world conditions. To achieve this, we have designed an emulation platform that can support physical and medium access control layers. The data communication at the application is based on the IEEE C37.118-2011-2 Standard. By considering a hierarchical network architecture for our testbed implementation, we propose an efficient method to reduce bandwidth, as well as provide capabilities for control and management at each hierarchical level. In addition, an efficient tree-based multihop routing protocol has been designed to match a specific distribution feeder structure. The testbed is then used to access different network configurations under various test conditions.

**Index Terms**—Distributed generation (DG) systems, Emulab, emulation, IEEE 802.11, phasor measurement unit (PMU), radial, synchrophasors, wide area monitoring system.

## I. INTRODUCTION

A MAJOR challenge for future wide area measurement systems is how to respond effectively to various disturbances in the next generation of power networks. The phasor measurement unit (PMU) that is capable of detecting angular stability is becoming one of the most important measurement devices for power system monitoring and control. This is mainly due to its unique ability to sample analog voltage and current waveforms in synchronization with a GPS-clock. For a wide area monitoring and control system, it is imperative to implement a network infrastructure capable of handling a large amount of real-time synchrophasor data arriving at the phasor

data concentrators (PDCs). As the grid system continues to scale up, analyzing the aggregated data at the control center will become a major undertaking.

Currently, PMUs are mainly considered for high-voltage power transmission and their deployment for low-voltage distribution systems, referred to as micro PMUs ( $\mu$ PMUs), is gaining momentum [1]. This is a consequence of the advances in sensor networks, anticipated low-cost  $\mu$ PMUs, and control technologies, which have made it possible to monitor reactive power and voltage levels in the distribution system [2]–[4]. The distribution grid normally operates at medium-to-low voltages and may include a large number of consumers, some of whom may have power generation and energy storage capabilities. Under these conditions, the main challenge is how to regulate voltage and control the reactive power. Voltage regulators are normally placed along the distribution feeder so that they can adjust the voltage to a desirable level (e.g., + or  $-5\%$  of the nominal voltage). For example, a capacitors bank can be used to compensate reactive power caused by the inductive load for controlling the voltage level. This would be at the expense of magnifying harmonics, which could make it difficult to estimate the line frequency, as well as measure the phase angle between voltage and current in order to measure the power factor (PF). To ensure that the distribution system will maintain the voltage at the required level, the reactive power (either capacitive or inductive) needs to be measured first and then adequately supplied by generators in the distribution system. With the help of a synchrophasor network this can be achieved in real-time by measuring the PF in the vicinity of the installed distributed generation (DG) system. For instance, the control management in the PF mode may require injecting reactive power in order to maintain the PF close to unity or keep the ratio of real power  $P$  to reactive power  $Q$  (i.e.,  $P/Q$ ) constant. In a centralized control management system without the support of an infrastructure network, this cannot be done efficiently, especially in the presence of a large number of micro-generation devices such as rooftop solar panels and micro-wind turbines. Bear in mind that these devices, via power electronic interfaces (inverters), can be used to inject power [5], [6]. Furthermore, new inverters (e.g., advanced inverters) are capable of injecting reactive power and compensating for harmonics in addition to their primary function of real-power conversion [6], [7].

Manuscript received May 15, 2014; revised October 3, 2014; accepted January 23, 2015. Date of publication May 19, 2015; date of current version August 19, 2015. Paper no. TSG-00443-2014.

The authors are with Advanced Network Technologies, National Institute of Standards and Technology, Gaithersburg, MD 20899, USA (e-mail: Gharavi@nist.gov; bhu@nist.gov).

Color versions of one or more of the figures in this paper are available online at <http://ieeexplore.ieee.org>.

Digital Object Identifier 10.1109/TSG.2015.2424196

The presence of multiple inverters in controlling the reactive power has been studied in [8] for radial distribution feeders. In [8], it has been shown that reactive power compensation at multiple points in a low-voltage distribution can greatly enhance the voltage profile. In general, the connection of the DG into a distribution system needs coordination with available voltage and reactive power control equipment in the system. Distributing reactive power to minimize power loss has also been reported in [9]–[11]. As the DG installation continues to increase and more utility customers generate their own power, distribution systems' dependency on communication for centralized control is becoming vitally important. Indeed, despite a tremendous number of published reports in open literature, to the best of our knowledge there is no cost-effective communication networking scheme for a centralized control system.

Therefore, in this paper we present a design and implementation framework of a scalable wireless network architecture suitable for distributed grid systems. The synchrophasor network has a hierarchical structure where PDCs at each hierarchical level collect phasor information. The aggregated data is then forwarded to the next hierarchical level, hence requiring a higher data transmission. In order to reduce the amount of data, we propose a data reduction scheme by removing redundant phasor information before transmission to the next PDC level. The scheme also includes a synchrophasor data classification methodology that would allow each PDC to identify faulted areas at the local level, thus reducing the computational and monitoring complexities at the control center. Another contribution in this paper is the emulation-based implementation of the hierarchical network.

We use an Emulab [12], [13] platform to build a flexible testbed to access various wireless network configurations under real-world conditions. For packet exchanges at the application layer, the synchrophasors communication is based on the C37.118 [14], [15] standard, which is built on the top of the user datagram protocol over Internet (UDP/IP) layers. For wireless medium access control (MAC) layer and physical (PHY) layer, we use extendable mobile *ad hoc* network emulator (EMANE) [16] to implement the testbed. Specifically, we consider the IEEE 802.11 Standard [17] for communication between PMU and PMU/PDC. We also present a routing scheme suitable for radial and closed loop distributed feeder systems. The testbed is then used to measure packet loss, latency, bandwidth, and queue size, for wide ranging scenarios.

This paper is organized as follows. Section II describes our network strategy for designing the hierarchical synchrophasors network. Section III presents the Emulab-based implementation of the synchrophasors testbed, including the wireless LAN (WLAN) design architecture and some of its inherent capabilities. Section IV describes test scenarios in the DG environment. Finally, Section V presents the results of test and measurement in terms of throughput and delay performances under various wireless channel conditions. This is then followed by final remarks and the conclusion.

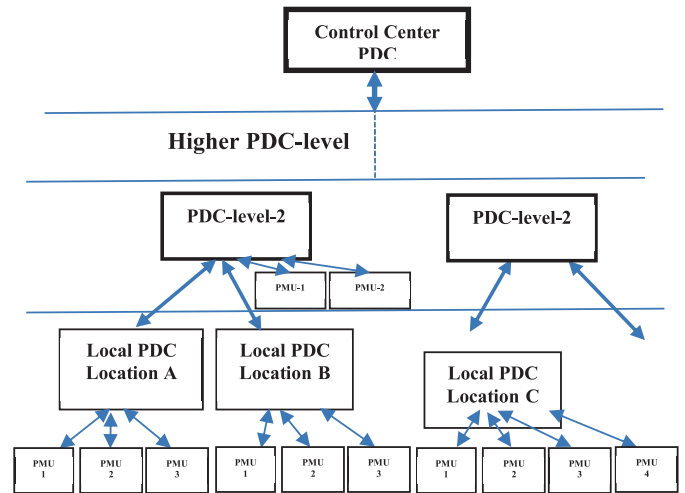


Fig. 1. Hierarchical PMU/PDC structure.

## II. HIERARCHICAL SYNCHROPHASOR NETWORK ARCHITECTURE

Currently, PMUs are mainly considered for deployment in high-voltage power transmission. Their expansion for deployment in the medium-to-low voltage in distribution systems is facing major challenges [1]. For example, these devices, which are referred to as  $\mu$ PMUs, should be able to measure the phase angles with much greater accuracy under severe noise conditions and in the presence of harmonics, which normally exist in distributed grid environments. While  $\mu$ PMUs are currently undergoing major advances to overcome these short-comings, our main objective is to design a network architecture that can be deployed not only in distribution feeders, but also in the transmission system.

### A. Hierarchical Network Architecture

Fig. 1 shows an example of a hierarchical synchrophasor network architecture, which has been considered in our implementation. As can be observed, PMUs in each region communicate with their local PDC. At the local PDC, the aggregated data is then forwarded to the next PDC level and this process continues until all data reaches the final PDC at the control center or distribution network operator (DNO). Note that in Fig. 1, the PMU-1 and PMU-2 are attached to the PDC-level-2 and communicate with PDC-level-2 either in LAN or in WLAN. PDC-level-2 collects data frames from PMU-1 and PMU-2, as well as combined data frame from local PDCs A and B. Based on the received information, it generates a larger combined data frame to higher level PDC. The data collected at the control center can then be archived for further processing, such as visualization and possible control/alarm actions for situational awareness.

To establish an end-to-end communication link between PMU/PDC and PDC, the first step would be to set up message communication at the application layer. The IEEE C37.118 Standard provides specifications for synchrophasor measurement (part-I) [14] and data formats for real-time communications (part-II) [15]. In addition, PDC

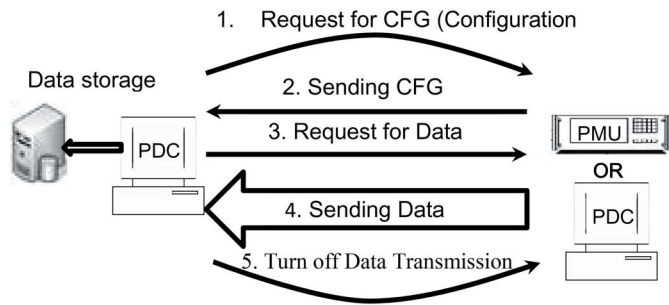


Fig. 2. Commands and data exchange between PDC and PMU/PDC.

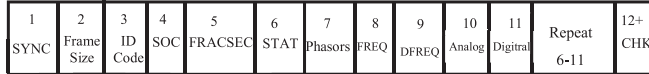


Fig. 3. Data frame structure.

requirements for power system protection, control, and monitoring are specified in [18], which includes requirements for synchronization, synchrophasor data processing, and real-time access. Fig. 2 shows commands and data exchange between a PDC and a PMU/PDC for real-time communication [15], [19].

The command frame is used to turn the transmission on or off. There are three configuration frame types, namely: 1) Configuration (CFG)-1; 2) CFG-2; and 3) CFG-3. CFG-1 provides information about the full capabilities of a PMU (i.e., reporting rates, frequency range, noise suppression, etc.). CFG-2 denotes the currently reported measurements. CFG-3 is optional and has a flexible frame format. Through the data frame, as shown in Fig. 3, a PMU transmits current and voltage amplitudes, their synchronized phasor angles, an estimated frequency, as well as a rate of change of frequency (ROCOF or DFREQ). The message also includes SYNC, frame size, identification code (i.e., ID Code), a time stamp, which is specified as a SoC and fraction of second (FRACSEC) of the received data frame, bit-mapped flags (STAT), analog data (ANALOG), digital data (DIGITAL), and CTC check bits (CHK).

When a PDC receives data from its multiple PMUs or lower level PDCs, it should first align the frame according to their time stamps. The time alignment is arranged in accordance with the SoC (SoC counts starting at midnight 01 Jan-1970) and FRACSEC of the received data frames. As shown in Fig. 4, a PDC has at least two sets of buffers for storing two consecutive data frames with the two time slots.

The first set of buffers stores the incoming data as it arrives and then sorts it according to their PMU/PDC ID [20]. Note that data frames from different PMUs may not always arrive at the same order and therefore the received data has to be reordered in the buffer accordingly. The second set of buffers corresponds to the data from preceding time slot. It contains the data that is transferred from the first set of buffers as soon all the data frames reach the PDC within a predefined time period. The second set of buffers also includes data that did not arrive on time (or lost) during the transmission of the previous time frame.

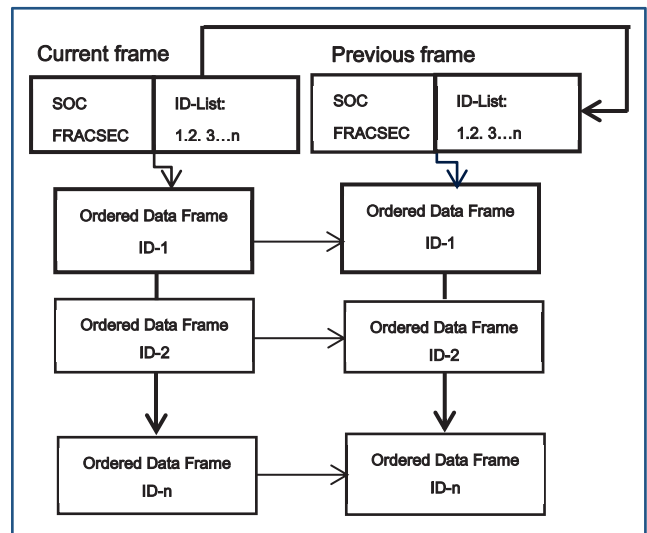


Fig. 4. Buffering structure to align and sort the data in accordance with a predefined list of source IDs at the PDC [note that the data frame can be received in a different order (First In First Out) depending on the transmission delay, which tends to change from time-to-time].

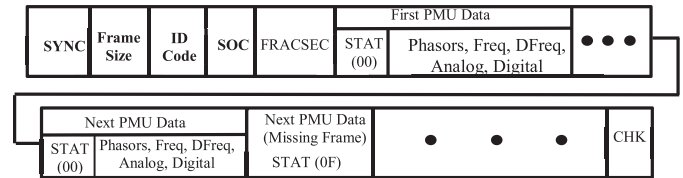


Fig. 5. Combined frame format which is generated at the local PDC for transmission to the next level PDC. Note that PMU data is placed in the order based on the previously received configuration frames.

As soon as a PDC receives data from its multiple PMUs, it will then forward it to the next level. To achieve this, the PDC will first construct a combined data frame that was received from its PMUs/PDCs with the same time stamp. The format of the combined frame is shown in Fig. 5. Packets arriving late or lost at the PDC are not included in the combined frame. The status of these packets is marked as "0F" (see Fig. 5).

It should be noted that the size of the combined frame increases at the next PDC level and continues to grow until it reaches the final PDC. Consequently, a higher level PDC would require more bandwidth for transmitting a combined frame to the next level. It should be noted that the synchrophasor data is reported on an  $N$  frames/s basis, where  $N$  can be selected between 1 and 120. Obviously, a higher frame rate would further accelerate a demand for more bandwidth. In addition, with deployment of a large number of PMUs in the serving area, analyzing the aggregated data at the final PDC located at the control center can become an enormous task.

In order to mitigate the computational burden at the control center, as well as reduce the transmission bandwidth at higher PDC levels, we propose a new scheme to overcome these shortcomings. Instead of adopting an increasing bandwidth setting, the proposed scheme removes redundant phasor information from the combined data frame before transmission to the next PDC level and hence does not need substantially more bandwidth at higher level PDC.

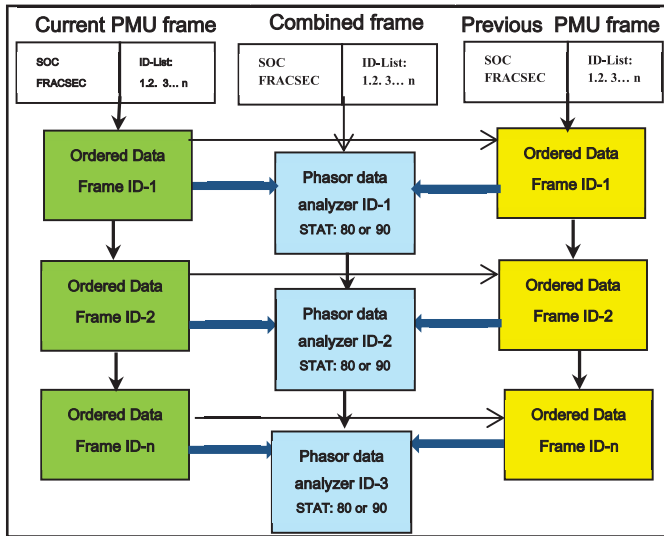


Fig. 6. Buffering arrangement for generating a combined data frame, which includes the synchrophasor data of abnormal nodes.

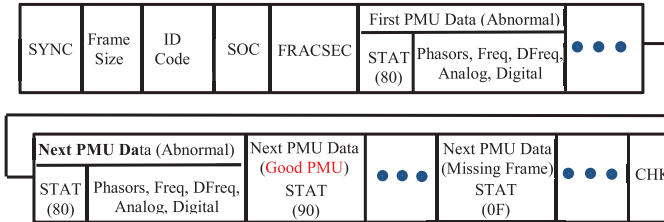


Fig. 7. Structure of a combined data frame for upper PDC, which includes only the synchrophasor data of the nodes that are classified as abnormal.

### B. Proposed Network Architecture

According to the C37-118-2011-2 [15], and as described in the previous section, a PDC generates a combined frame as soon as the predefined time period is reached. These data frames are collected in the PDC buffer and then rearranged in an order based on the previously received configuration frames. Our objective is to eliminate the redundant data received from the lower level through some processing at the local PDC. Therefore, in the proposed distributed-monitor-control scheme, that uses PMU classification at the PDC level, the combined frame will only include data for those nodes that undergo transitional changes. To accomplish this, a local PDC checks and compares its synchrophasor data with the measurements in the previous report (note that this information is readily available as it is stored in the PDC buffers) to assess the conditions of the nodes in its region. The assessment can be based on certain criteria such as frequency, ROCOF, PF, etc. For instance, if PMU frequencies are stable and the phase difference remains the same as the previous measurements, the local PDC modifies the corresponding PMUs STAT from (00) to (90) without having to include the measured data (e.g., phasors, freq, dfreq, analog, and digital) when generating its combined data frame for transmission to next PDC level. Figs. 6 and 7 show the new PDC buffering arrangement to construct a combined frame. As shown in Fig. 7, the combined frame will include only the synchrophasor data of the nodes that are classified as abnormal with STAT: 80.

Obviously, in a situation where a data frame is lost or did not arrive on time, such a classification cannot take place. Under these conditions, the status of the node can be classified as unknown (STAT: A0) until two consecutive data frames become readily available in the PDC buffers. Alternatively, with adding more sets of buffers, the classification can be done using data from the two nearest time slots stored in the PDC buffers. In our implementation, we increased the number of buffer sets up to 10 in order to reduce the number of nodes with unknown status.

Once the next level PDC (above the local PDCs) receives the new combined frame from its regional PDCs, it can then identify the locations of the abnormal nodes and subsequently the lines or feeders that connect them. As a result, the regional PDC can have the capability to initiate any necessary action such as islanding, injecting reactive/real power, or some other protective actions. Estimating the PF at the local PDC can also contribute to controlling the power.

### C. PF Measurement

The PF is a good indicator of how effectively the current is being used in the supply system. Currently, the PF calculation is not a part of IEEE C37.118 measurements, but in a DG network PF can play a crucial role in controlling the reactive power by keeping, for instance, the PF close to unity. Bear in mind that, distribution systems have reactive power present due to inductive loads. The inductive reactive power, which is measured in volt-amperes-reactive (VAR), causes the current to lag behind the voltage in phase. On the other hand, the voltage across a capacitor will oppose this change, causing the current to lead the voltage. When power systems have purely resistive loads, the power is called real power and is measured in watts. The reactive power and the real power represent a complex power where the imaginary axis and real axis correspond to the reactive power and real power of the vector diagram, respectively. Apparent power is the magnitude of the complex power in kilovolt-amperes (kVA), and the ratio between active power and apparent power represents the PF. In the vector diagram, PF is defined as:  $PF = \cos \varphi_{v,i}$ , where  $\varphi_{v,i}$  is the phase angle difference between voltage and current and can be measured by/from the synchrophasor data.

For instance, the phase difference can be calculated at each measurement site, which could then be assessed at the local PDC or control center for possible PF correction. For inductive loads, PF correction can be achieved using capacitors to compensate for the inductive component of the current. Bear in mind that the capacitive and inductive loads could cause oscillation. In addition, calculation of the PF using the cosine of the angle difference between the voltage and current is based on the assumption that both waveforms have only fundamental frequency components. In the presence of harmonics, the calculation for a single phase can be done by measuring what is called true PF (TPF), which takes into consideration the harmonic distortion of voltage and current waveforms [21]–[23].

We should point out that we assume the  $\mu$ PMUs are capable of measuring the phasors of voltage and current with

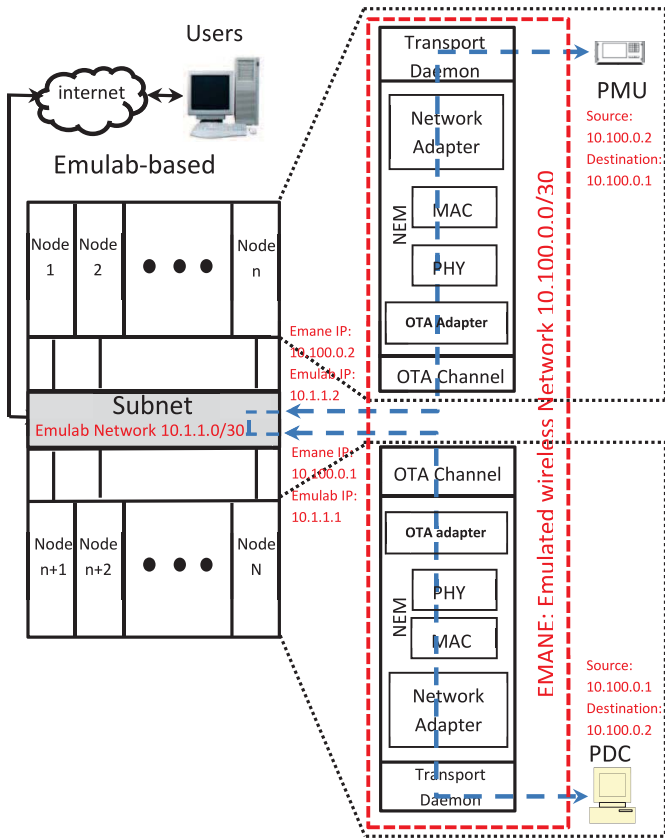


Fig. 8. Emulab-based network set up for communication between PMUs and PDCs.

high precision. In addition, the  $\mu$ PMUs should also be able of estimating the fundamental frequency and harmonics with great accuracy. This would require using efficient phase and frequency estimations. This can be very challenging, especially in distributed systems due to the presence of excessive noise and harmonics. In our testbed implementation, we have used a recursive discrete Fourier transform [24]. Based on the synchrophasor data, the local PDC then calculates the TPF. In our DG model (see Fig. 9), the  $\mu$ PMUs are placed near the inverters or other sensitive locations, such as reclosers and tie breakers.

### III. EMULATION-BASED WIRELESS TESTBED IMPLEMENTATION

In our implementation so far, we have considered UDP/IP. Compared with TCP/IP, UDP/IP is much simpler and more suitable for real-time transmission. For an end-to-end transmission of synchrophasor data over WLAN, it is very important to select an appropriate set of tools for performance testing. Bear in mind that using hardware to implement a testbed for wireless applications imposes a significant challenge in terms of cost, effort, time consumption, and more importantly, a lack of flexibility for modifying network configurations, as well as their evaluations under various test conditions. On the other hand, a combination of simulation and emulation leverages a common platform for real-time experimentation. Indeed, emulators can be effective tools to design a network at the implementation stage. Such a testbed

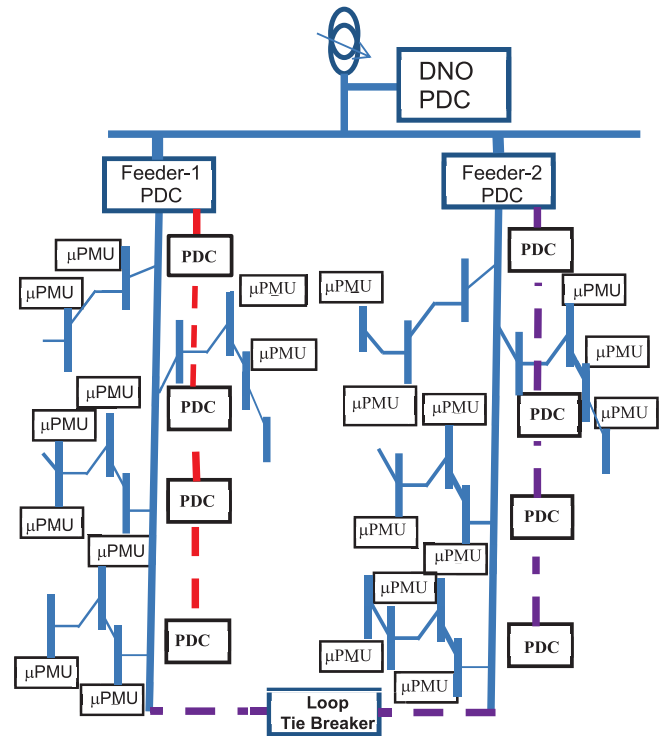


Fig. 9. Example of loop-radial for wireless network structures consisting of local  $\mu$ PMUs communicating to the DNO PDC through their local PDC.

would allow us to assess the suitability of different network configurations for local and wide area measurement systems. Our primary goal is to implement the hierarchical network described in the previous section. To accomplish this, we use Emulab [12], [13] and EMANE [16] to construct PHY and MAC layers to emulate a wireless connection between PMUs and a PDC.

Our testbed comprises 29 Emulab nodes where each can be configured to represent either a PMU or a PDC. This provides a great deal of flexibility to construct different network configurations of PMUs and PDCs. Every node (PDC or PMU) is accessed via a 100 Mb/s Ethernet link as shown in Fig. 8. In order for each node to function as a WLAN device, such as IEEE 802.11, we use EMANE [16]. EMANE is an open source framework with a set of application program interfaces (APIs) and supports creating MAC and PHY layers to function in emulation environments. A logical component of EMANE is the network emulation module (NEM) that establishes MAC and PHY for WLAN experiments. The complete set up and the role of EMANE in setting up the interfaces for a wireless connection between PDC and PMU are shown in Fig. 8. As shown in Fig. 8, the NEM provides a virtual interface to the over the air (OTA) channel, which is part of the EMANE domain. A NEM is also responsible for transferring data between the emulation and application domains. This is done by creating a virtual interface to the transport layer that can route traffic within the emulation domains. Fig. 8 also shows the structure of communication link and the role of EMANE in setting up the interfaces for wireless connections between PDCs and PMUs.

It should be noted that the EMANE runs on each PC with its own IP address to represent an IEEE 802.11-based WLAN device. To establish a peer-to-peer multihop communication between a PMU/PDC and a PDC, the IEEE 802.11 is set to operate in a distributed coordination function (DCF) mode [17]. It should be noted that the IEEE 802.11 Standard uses a carrier sense multiple access with collision avoidance access protocol. The protocol controls access to the shared wireless medium [17], which makes it very sensitive to the interference caused by real-time data transmission [25] as well as by other active nodes [26]. In addition, the collision avoidance method operates in half-duplex to prevent interference by simultaneous transmission and reception by the same node.

#### IV. NETWORK DEPLOYMENT IN DISTRIBUTED GENERATION

The PMUs collect measurement data throughout the power system, which may include generation, transmission and distribution. The synchrophasor data consist of amplitudes of voltage and current and their respective phase angles and are time stamped using a GPS signal that is the same at every location. Based on these measurements the phase difference between the current and voltage can then be used to calculate PF (or TPF with harmonics). From the synchronized measurements between two locations at the same time instant, it is possible to assess the system stress conditions in the presence of loads and inverters.

Bear in mind that in DG environments the PF can be regulated by injecting active and reactive powers in order to maintain the voltage level within an acceptable range. Unlike the transmission grid, which has a meshed structure, the distribution system generally has a radial or, in some rare cases, a loop structure (note that in a loop structure a node can be fed from two directions). In the presence of the generators, the injected power can cause severe problems such as voltage rise. For voltage control over the radial feeder, the on-load tap-changer (OLTC) at the transformer is normally considered. In the absence of any communication infrastructure using OLTC may not be sufficient enough to control the voltage level and reactive power [27]. With the support of communication networks, reactive power can be controlled remotely using a capacitor bank at the local control center [8]–[11]. Within the centralized scenario, if the synchrophasor information throughout the distributed feeder is made available at the DNO, the controller would then be able to instruct power injection from generators/inverters that are nearest to the loads with high demand by analyzing the data in each local area. Fig. 9 shows an example of two radial feeders with  $\mu$ PMUs placed at such sensitive locations. We assume the final PDC at the DNO (DNO-PDC) is connected to both feeder PDCs via the substation backbone network. In this figure, we presume the measurement devices (e.g.,  $\mu$ PMUs) are placed in the vicinity of the generators/inverters, as well as nearby loads and/or secondary transformers.

To provide a wireless communication link throughout the feeder, we are considering a tree-based multihop routing protocol [26], [28], [29]. Our proposed tree-like routing

scheme is based on the optimized link state routing (OLSR) protocol [30]. The OLSR is a proactive routing protocol developed for mobile wireless networks. This protocol maintains a routing table by periodically exchanging topology information in the network. For our application, however, since all the PMUs are installed at fixed locations, the network topology does not need to be updated on a regular basis, but only in situations when the network topology undergoes some changes (e.g., new PMUs are added). Before describing our routing scheme, the following presents a brief description of the OLSR.

##### A. Optimized Link State Routing Protocol

OLSR is an optimization of a pure link state protocol that employs multipoint relays (MPRs) to reduce the number of control messages transmission in the network. A MPR node is selected by its one-hop neighbors and its function is to forward control messages. Every node periodically broadcasts a “HELLO” message in order to create its neighbor table, as well as select its MPRs. This message includes a list of symmetric neighbor nodes with bi-directional link and a list of heard-only neighbor nodes with unidirectional links. If a node finds itself in a HELLO message, it validates the sender node as a bidirectional neighbor. By exchanging HELLO messages each node collects its neighbors’ information for up to two hops. Based on such information, nodes choose and list their MPRs. The MPRs are selected in such a way that all the two-hop neighbors are covered while the number of MPRs would be small enough to achieve a reduction of network overhead. Upon receiving a HELLO message that includes the MPR information, each node generates its MPR table containing the selected MPRs.

To construct a topology table for routing packets each MPR periodically broadcasts a topology control (TC) message to announce its MPR selector list. The information contained in the message is flooded and diffused throughout the entire network so that every node can build its topology table. An entry in the topology table contains the destination node and its last hop node to that destination (i.e., pairs of {node, last hop}), corresponding to an MPR selector in the received TC message and the originator of the TC message.

Based on the neighbor and topology table, a node can then calculate and generate its routing table. The table entries consist of destination node, next hop address, and estimated distance from the destination (e.g., hop-count). Specifically, any connected pair of {node, last hop} in the topology table is used by a node to find a path to the destination. For instance, if a node wants to find a route to destination  $R$ , it first finds a pair of  $(R, I)$  and then a pair of  $(I, N)$  and if  $N$  is listed as its neighbor, the routing is established. Otherwise, the process will continue. By selecting a pair with minimal distance (hop count), nodes are capable of finding an optimal route to their destination. Note that every known destination node has a corresponding entry in the routing table.

##### B. Proposed OLSR-based Tree Routing Protocol

Because of the tree-like structure of radial feeders, OLSR is tailored to develop our OLSR-based tree

routing (OTR) protocol. As opposed to OLSR where every node broadcasts a TC message, the OTR only allows specific nodes such as feeder-1 and feeder-2 PDCs (see Fig. 9) to generate and broadcast a TC message. This would considerably reduce implementation complexities, as well as transmission overhead. A TC message is generated and broadcast by both feeder-1 and feeder-2 PDCs in a similar manner as the root announcement in hybrid wireless mesh protocol (HWMP) of 802.11s [29]. The information extracted from the received TC message is used to create a routing table entry. The originator of the received TC message (i.e., feeder-1 or feeder-2 PDCs) is labeled as the destination while the hop count in the received TC message is used as the distance to each destination (i.e., feeder-1 or feeder-2 PDCs). Therefore, as soon as a node receives a TC message, it creates its routing table (instead of topology table). Note that due to a simple tree-like structure of radial feeders, compared with the HWMP mesh networks [27], there is a limited number of choices to find an optimal route. This would help to eliminate computation complexity which would otherwise be needed to find pairs with minimal distance. Through rebroadcasting a TC message by MPRs all nodes in the network are able to create route entries in feeder-1 and feeder-2 PDCs.

In order to help both feeder PDCs to learn and establish routes to all nodes in the network, a new control message called reply to TC (RTC) is created and used in the proposed OTR. After creating route to feeder-1 or feeder-2 PDCs, a node upon receiving a TC message, unicasts a RTC to the sender of the TC message by labeling the feeder-1 or feeder-2 PDCs as the destination with itself as the originator. This RTC is then forwarded to the destination (feeder-1 or feeder-2 PDCs) by intermediate nodes along the path based on their routing tables. In this way, feeder-1 and feeder-2 PDCs can generate route entries to all nodes in the network. Note that the RTC message is only a slight modification of the TC message, where a new destination field (feeder-1 or feeder-2 PDCs) and a new receiver field (receiver is selected based on routing table) are added.

The proposed routing protocol has been implemented and included in our Emulab testbed. As will be shown in the simulation section, it considerably improved the overall network performance compared with OLSR.

As can be observed from Fig. 9, the  $\mu$ PMUs are distributed along every subfeeder, for volt/VAR assessment. These  $\mu$ PMUs report to their local PDC which will then generate a combined frame for transmission to the feeder PDC by hopping through other local PDCs along its way. We point out that both radial feeders, as shown in Fig. 9 with dashed lines, can be tied together to form a closed loop [31], [32].

Looping the radial feeders through a tie breaker switch would allow the utilities to take advantage of closed loop by turning the tie breaker switch on when needed. This is considered the most cost effective solution for future upgrades [30]. For example, under normal conditions the two feeders from the same transformer can form a closed loop. In abnormal situations the tie breaker can be switched off so that feeders can operate in radial fashion until the abnormal areas where the fault occurred have been cleared. Although we have made

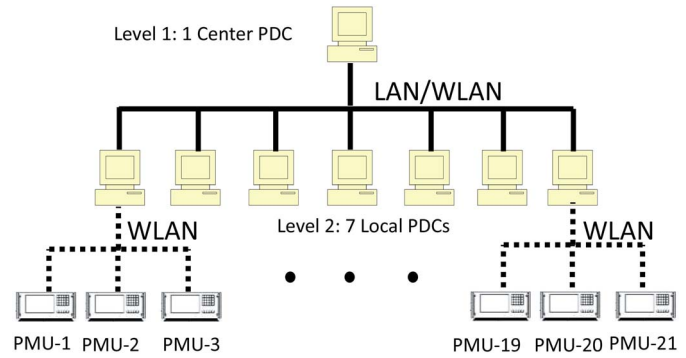


Fig. 10. Hierarchical config.-1. There is one central PDC in level 1, seven local PDCs in level 2, and 21 PMUs attached to these seven local PDCs. PMUs communicate with local PDCs in single hop mode.

no attempt to investigate the effect of a tie breaker in the loop, our network can be easily modified to include a sensor that can provide a wireless link for any control action to open and close the tie breaker switch.

## V. SIMULATION RESULTS

Having completed the implementation of a real-time testbed using the emulation platform, in this section, we present the performance of hierarchical PMU networks. The Emulab system is employed, which consists of 29 PC nodes, where every PC is preinstalled with UBUNTU version 12 [33] and a node can be either PDC or PMU. The Emulab network operates at 100 Mb. To implement a WLAN, we use the EMANE to set up links between PMUs and PDCs. The IEEE 802.11 wireless link is considered for the testbed and is set to operate in a DCF mode. The OLSR [30] and the proposed OTR protocols are invoked for multihop communication. The wireless link's bandwidth is set to operate at 2 Mb. The noise figure is 4.0 dB and the frequency is 2.4 GHz. The retransmission limit is set as 1, based on the consideration that when a packet is lost it may not be necessary to retransmit it since the data packet with next time stamp is expected to arrive via the next data frame. In our simulation, free space and two ray channel propagation models are used. The message exchanges at the application layer are based on the C37.118 Standard. In addition, we have modified the C37.118 frame structure in order to include our proposed PMU node classification scheme at the PDC level (see Section II).

Three hierarchical network configurations are exploited, namely config.-1, config.-2, and config.-3. The corresponding network configurations are shown in Figs. 10–12, respectively. As can be seen from Fig. 10, there is one central PDC in levels 1 and 7 local PDCs in level 2. Each local PDC manages three PMUs and hence there are 21 PMUs in total. At the PHY layer, communication amongst PMUs and local PDCs is accomplished through 802.11b WLAN with a 2 Mb bandwidth. Two scenarios are considered for PHY layer communication between PDCs at the last stage. In scenario A, communication between PDCs is through wired LAN with 100 Mb bandwidth, while in scenario B the connection is done via 802.11b WLAN with 2 Mb bandwidth.

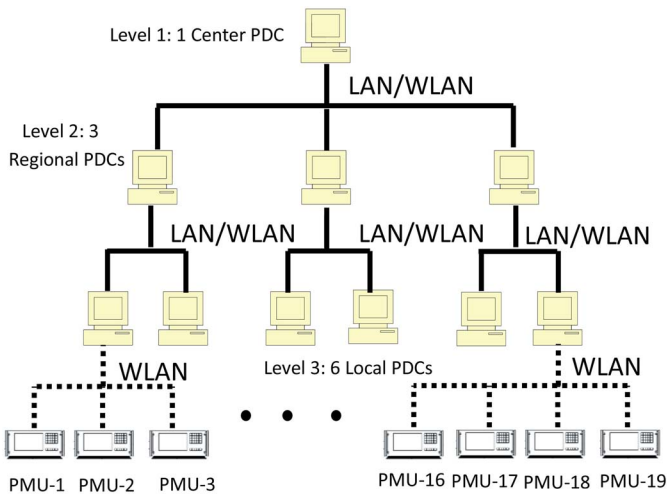


Fig. 11. Hierarchical config.-2. There is one central PDC in level 1, three regional PDCs in level 2, six local PDCs in level 3, and 19 PMUs attached to these six local PDCs. PMUs communicate with local PDCs in single hop mode.

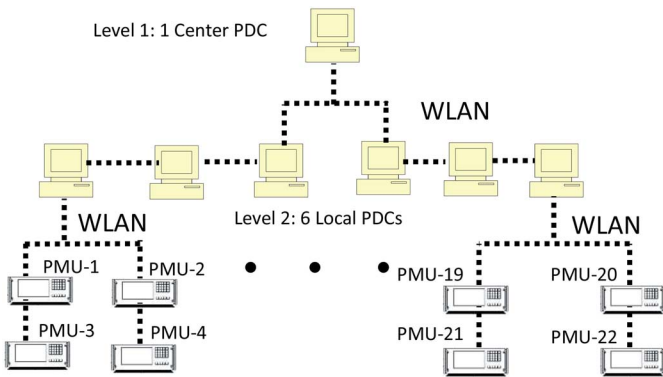


Fig. 12. Hierarchical config.-3. There is one central PDC in level 1, six local PDCs in level 2, and 22 ( $4 \times 4 + 2 \times 3$ ) attached to the six local PDCs. PMUs communicate with local PDCs in multihop mode.

Config.-2 (see Fig. 11), consists of one central PDC in level 1, three regional PDCs in level 2, and six local PDCs in level 3. Altogether, there are 19 PMUs, which are controlled by six local PDCs. Similar to config.-1, scenarios A and B are considered, where the communication between PDCs is either through 100 Mb wired LAN, or 802.11b WLAN with 2 Mb bandwidth, respectively.

Config.-3 is specifically designed to implement network deployment in a DG scenario (see Fig. 9). As opposed to config.-1 and config.-2 where communication between PMUs and PDCs is operated in single hop mode, config.-3 communications are in multihop mode. Specifically, in config.-3, PMUs report to their local PDC by hopping through other PMUs while local PDCs forward combined frames to the central PDC by hopping through local PDCs along the way. As seen in Fig. 12, we have one central PDC in level 1, six local PDCs in level 2, and 22 attached PMUs.

In our tests and evaluations, we use the IEEE C37.118 Standard for synchrophasor data transfer between PMUs/PDCs and PDCs, as well as our proposed distributed-monitor-control scheme, which uses PMU classification at the PDC level. The latter is developed by

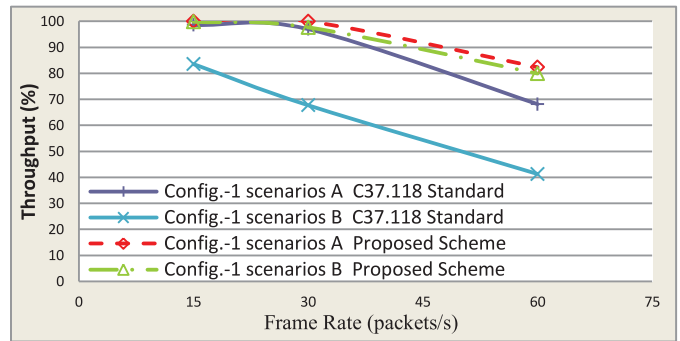


Fig. 13. Throughput performance evaluations of the proposed distributed-monitor-control scheme and the IEEE C37.118 Standard in config.-1 scenarios A and B.

modifying the IEEE C37.118 Standard in order to reduce the system overhead, share the computational burden of the central PDC and hence improve the throughput and average end-to-end delay performance. As described in Section II, in the proposed scheme a local PDC compares and then classifies the received data from its PMUs. This is done with the help of multiple buffer sets. Therefore, a PDC is capable of storing and comparing at least two consecutive data frames from its PMUs. By comparing these data the PDC can then detect abnormal PMUs. Currently, we use a change of frequency (within a certain range) as a criterion for a PMU classification. For DG systems, we also include the PF measurement at each PDC level in order to assess the amount of reactive and active power that is needed to be injected or absorbed by local inverters and generators.

As shown in Fig. 7, in the combined data frame from local PDCs to the central PDC the measurements of abnormal PMUs are included with STAT being 80, while the measurements of good PMUs are flagged with a STAT of 90. However, in order to provide the good PMUs data in the central PDC archive, local PDCs will include these PMUs measurements in the combined data at regular intervals (e.g., every 1 s). Note that in our simulations model, every PMU has five phasors, three analog values, and one digital value. The packet size of the data frame is 80 bytes. All the packets are transferred in a UDP-based data transfer protocol. The fundamental frequency of synchrophasor measurements is 60 Hz. A set of data frame rates, namely 15, 30, and 60 frames/s, is used to evaluate the schemes' performance.

#### A. Comparison of the Proposed Distributed-Monitor-Control Scheme and the IEEE C37.118 Standard

In Figs. 13 and 14, we assess the throughput and delay performances for the proposed distributed-monitor-control scheme using the PMU classification at each PDC and the IEEE C37.118 Standard in config.-1, which are referred to as scenarios A and B. It can be seen from Figs. 13 and 14 that the proposed PMU node classification scheme shows superior performance when compared with the IEEE C37.118 Standard, both in terms of throughput and delay. This is particularly true for scenario B where the IEEE 802.11b wireless link is employed for communication between PDCs, and

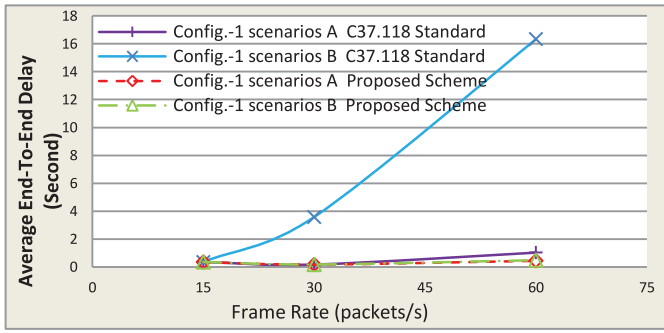


Fig. 14. Average end-to-end delay performance evaluations of the proposed distributed-monitor-control scheme and the IEEE C37.118 Standard in config.-1 scenarios A and B.

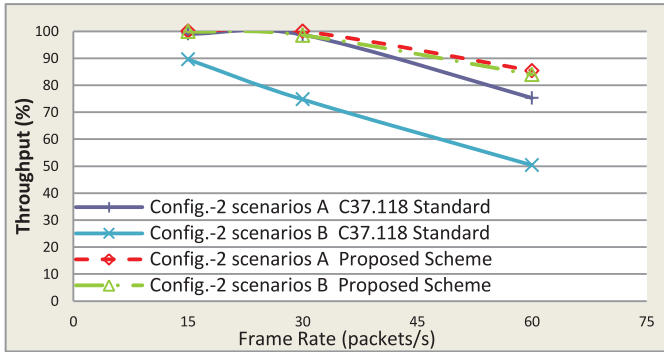


Fig. 15. Throughput performance evaluations of the proposed distributed-monitor-control scheme and the IEEE C37.118 Standard in config.-2 scenarios A and B.

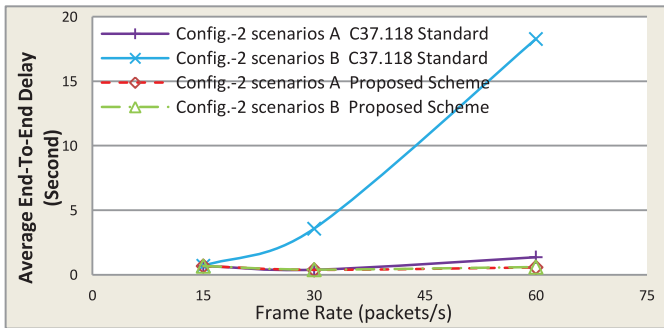


Fig. 16. Average end-to-end delay performance evaluations of the proposed distributed-monitor-control scheme and the IEEE C37.118 Standard in config.-2 scenarios A and B.

the proposed scheme achieves a considerable gain over the IEEE C37.118 Standard. This is mainly because of the greatly reduced packet size of the combined data frame. This has also contributed to mitigating the co-channel interference as a higher data rate contributes to the effect of co-channel interference. It can also be easily deduced from Figs. 13 and 14 that both schemes perform better in scenario A than the scenario B. This is due to the fact that at the final stage, the wired LAN is used for scenario A to transmit the aggregated data, which requires a much higher bandwidth. In contrast, in scenario B where the IEEE 802.11b is used, the transmission suffers greatly from co-channel interference.

For config.-2, Figs. 15 and 16 show the throughput and delay performance for both schemes under the same

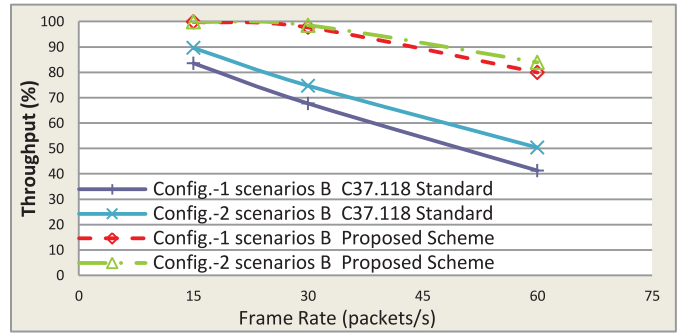


Fig. 17. Throughput Performance comparisons of the proposed distributed-monitor-control scheme and the IEEE C37.118 Standard in scenario B of config.-1 and config.-2.

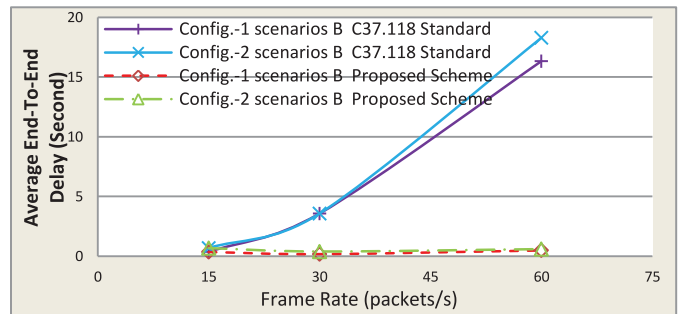


Fig. 18. End-to-End Delay Performance comparisons of the proposed distributed-monitor-control scheme and the IEEE C37.118 Standard in scenario B of config.-1 and config.-2.

transmission conditions. As could be expected, the proposed PMU classification scheme outperforms the IEEE C37.118 Standard in terms of throughput and delay for both scenarios. This is also verified by looking at Figs. 17 and 18, where the performances of the PMU classification scheme in config.-1 and config.-2 are evaluated comparatively. We can observe that the proposed scheme attains a very close performance in both configurations. In contrast, the IEEE C37.118 Standard's performances for both configurations are relatively similar.

We should point out that the main feature of the hierarchical structure is to allow the PDC to provide an assessment of the grid at a local level rather than at the control center. Consequently, this reduces not only the computation, but also decision making complexities at the main control center. Although this would be at the expense of greater bandwidth at higher PDC levels, thanks to the bandwidth reduction scheme presented in this paper, the local PDC have the ability to assess the voltage level and reactive power at the each PDC level. More importantly, the reduction of data rate would allow, for instance, more PMUs to report to the local PDC and/or increase the number of hierarchical levels as long as the aggregated data rate at the highest PDC level remains within the bandwidth capacity of the WLAN device. As shown in Figs. 13 and 15 for both scenarios A and B, the data rate remains within the IEEE 802.11b capacity even at the highest PDC level.

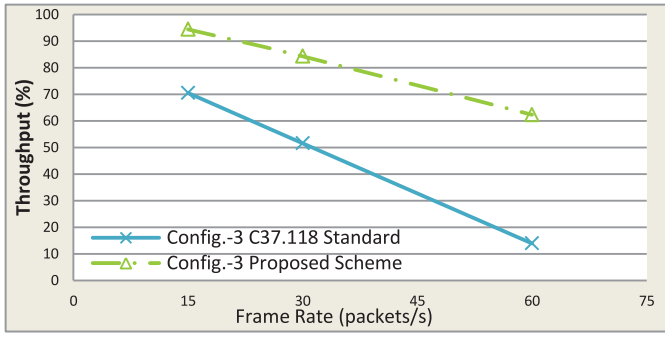


Fig. 19. Throughput Performance evaluations of the proposed distributed-monitor-control scheme and the IEEE C37.118 Standard in config.-3.

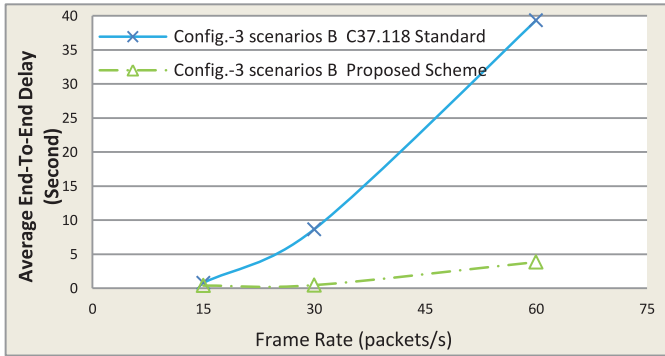


Fig. 20. Average End-to-End Delay Performance evaluations of the proposed distributed-monitor-control scheme and the IEEE C37.118 Standard in config.-3.

**B. Investigation of the OLSR and OTR Protocols**

In Figs. 19 and 20, a multihop scenario of config.-3 is investigated, where the OLSR protocol is employed as a proactive routing protocol for multihop communication. Different from the single hop communications in config.-1 and config.-2, multihop communications generates more co-channel interference when a similar number of PMUs and PDCs are deployed. Therefore, both schemes' performances degrade correspondingly in config.-3. However, compared to the IEEE C37.118 Standard, the proposed scheme demonstrates its robustness with much less degradation in this configuration, due to the benefit of less overhead. Obviously, the proposed distributed-monitor-control scheme is indispensable when implementing network deployment in DG. The proposed OTR protocol is investigated and compared with the OLSR in Figs. 21 and 22. The proposed OTR protocol achieves a noticeable improvement over the OLSR, because of the benefit of significantly reduced network overhead. Furthermore, in the tree-like multihop scenario of config.-3 the proposed OTR protocol achieves the advantage of much less complexity over the OLSR protocol.

**C. Impact of the Number of Buffer Sets**

We should point out that in the previous results, we employ five sets of buffers at the PDC to store and classify the received data frame. In Figs. 23 and 24, different numbers of buffer sets are deployed to access impact on the systems performance. Bear in mind that in a situation where the previous

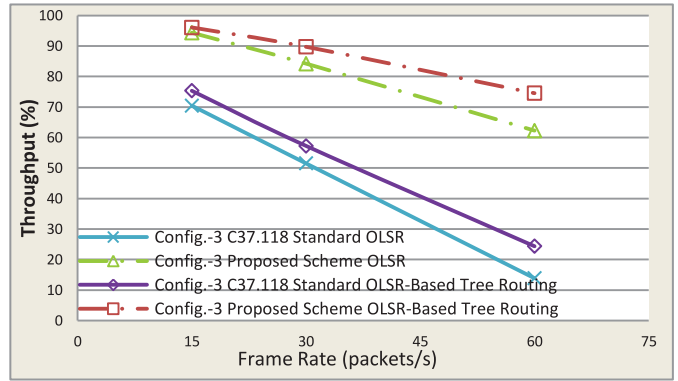


Fig. 21. Throughput performance evaluations of the proposed OTR protocol and the standard OLSR in config.-3.

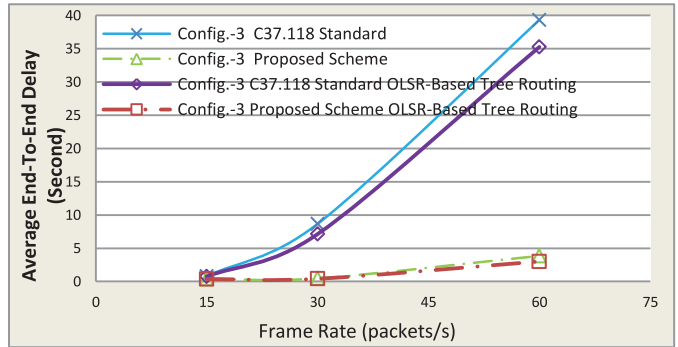


Fig. 22. Throughput performance evaluations of the proposed OTR protocol and the standard OLSR in config.-3.

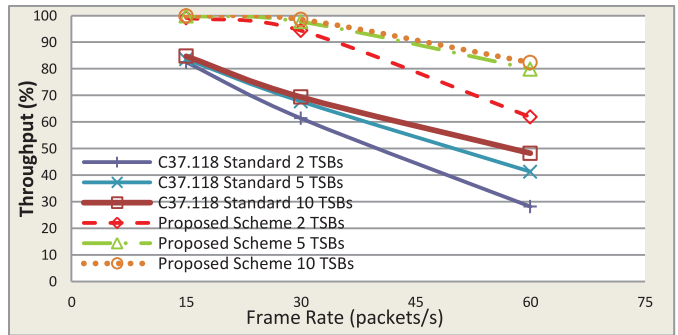


Fig. 23. Throughput performance comparisons of the proposed scheme and the IEEE C37.118 Standard using different numbers of buffers in config.-1 scenario B.

data has been lost due to unreliable wireless transmission, PMU node classification cannot be carried out. However, by adding more buffer sets, the PDC would be able to use the nearest available data frame stored in the buffer set. As can be seen, the performance of the proposed scheme is further improved, as compared with the IEEE C37.118 Standard. For instance, Figs. 23 and 24 depict the results by employing the number of buffer sets to 2, 5, and 10. These results indicate that by increasing the number of time slots associated with each set of buffers, the performance can be further enhanced. Under poor wireless channel conditions, we can expect this gap to grow further.

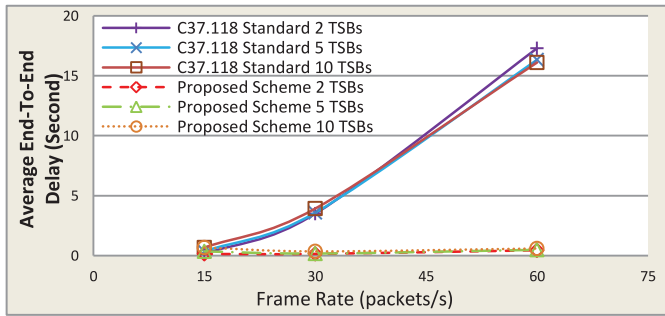


Fig. 24. Average end-to-end delay performance comparisons of the proposed scheme and the IEEE C37.118 Standard using different numbers of buffers in config.-1 scenario B.

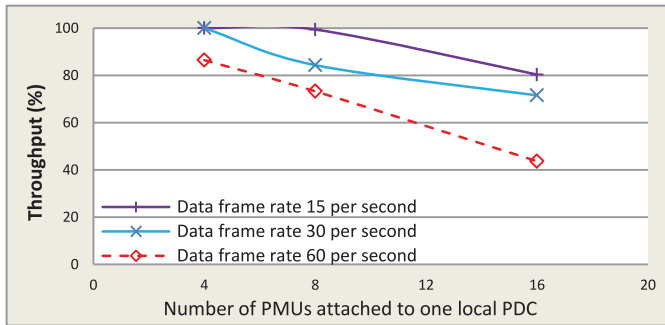


Fig. 25. Throughput performance evaluations on the communication between PMUs and local PDCs, where one local PDC and different numbers of attached PMUs are considered.

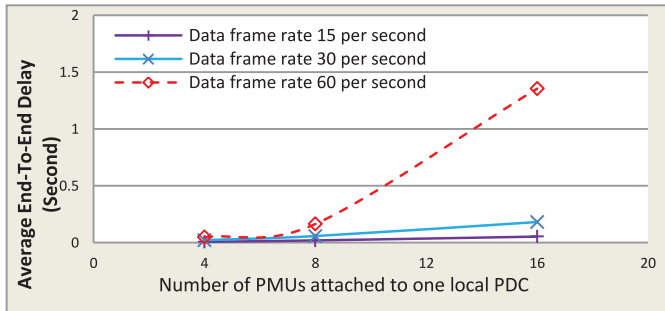


Fig. 26. Average end-to-end delay performance evaluations on the communication between one local PDC and different numbers of attached PMUs.

#### D. Investigation on the Communication Between PMUs and Single PDC

In our next set of experiments, we focus our investigation on the communication between PMUs and a single PDC, where a PDC communicates with different numbers of PMUs. The main purpose of this experiment is to assess the impact of using a higher number of PMUs reporting to a single PDC in wireless environments. The results are shown in Figs. 25 and 26, which indicate that when the data frame rate is at 30 packets per second or higher, the performance degrades significantly as the number of PMUs exceed 8. This is due to the effect of co-channel interference for transmission over a 2 Mb IEEE 802.11b wireless link. According to these results, we can conclude that the number of PMUs reporting to a PDC should be less than 8.

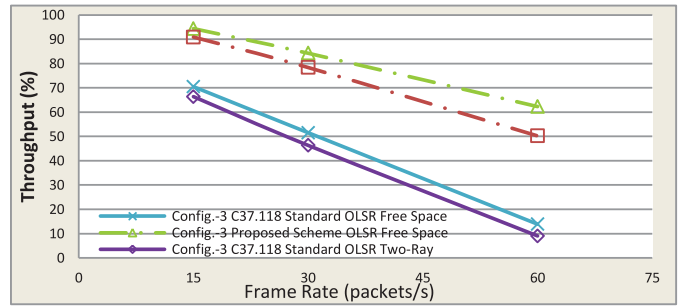


Fig. 27. Throughput performance evaluations of the proposed scheme with free space and two ray channel models in config.-3.

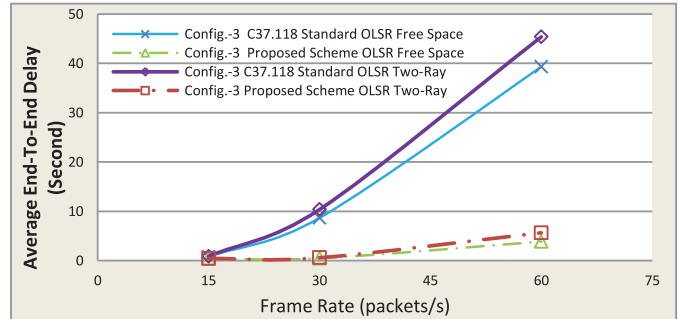


Fig. 28. Average end-to-end delay performance evaluations of the proposed scheme with free space and two ray channel modes in config.-3.

Finally, we should point out that in contrast to previous simulations where a free space channel model is used, Figs. 27 and 28 employ a two ray channel mode with average 3 dB lognormal shadowing for investigation and comparison. The proposed scheme gets a worse performance in a two ray channel mode. As expected, this would affect the overall throughput performance.

## VI. CONCLUSION

Our objectives in this paper were to design a hierarchical synchrophasor network for distributed grid systems and then implement a testbed using an emulation platform to assess the network under a real-world experimentation environment. The network has a hierarchical structure where PMUs initially communicate with their local PDC. The local PDCs can then forward the aggregated information to the next level PDC and so on. The number of hierarchical levels depends on the control strategy and the placement of the synchrophasor devices throughout the distribution feeder. The main problem with the hierarchical network is that the size of the data can grow rapidly at each higher level PDC. A data reduction method was then proposed. The new scheme would allow the PDC at each level not only act as a local controller, but also considerably reduce the information that is needed to be transported to the next level.

We used Emulab to implement the testbed. The testbed is then used to assess different network configurations under various test scenarios. This also included a scenario for radial and closed-loop feeders in a DG environment. A tree based routing has then been proposed for the DG system. The results indicate that the PDC data classification method cannot only

mitigate redundant data, but can also assist the PDC at each level to monitor and control the grid locally.

#### ACKNOWLEDGMENT

The authors would like to thank Dr. Gerald FitzPatrick from NIST for his constructive comments and support.

#### REFERENCES

- [1] A. Von Meier, D. Culler, A. McEachern, and R. Arghandeh, "Micro-synchrophasors for distribution systems," in *Proc. IEEE Innov. Smart Grid Technol. Conf. (ISGT)*, Washington, DC, USA, 2013, pp. 1–5.
- [2] H. Nazari-pouya and S. Mehraeen, "Optimal PMU placement for fault observability in distributed power system by using simultaneous voltage and current measurements," in *Proc. IEEE Power Energy Soc. Gen. Meeting*, Vancouver, BC, USA, Jul. 2013, pp. 1–6.
- [3] J. Liu *et al.*, "Trade-offs in PMU deployment for state estimation in active distribution grids," *IEEE Trans. Smart Grid*, vol. 3, no. 2, pp. 915–924, Jun. 2012.
- [4] M. Wache and D. C. Murray, "Application of synchrophasor measurements for distribution networks," in *Proc. IEEE Power Energy Soc. Gen. Meeting*, San Diego, CA, USA, Jul. 2011, pp. 1–4.
- [5] F. Katiraei and M. R. Iravani, "Power management strategies for a micro-grid with multiple distributed generation units," *IEEE Trans. Power Syst.*, vol. 21, no. 4, pp. 1821–1831, Nov. 2006.
- [6] M. Prodanovic, K. De Brabandere, J. Van den Keybus, T. Green, and J. Driesen, "Harmonic and reactive power compensation as ancillary services in inverter-based distributed generation," *IET Gener. Transmiss. Distrib.*, vol. 1, no. 3, pp. 432–438, May 2007.
- [7] M. E. Baran and I. M. El-Markabi, "A multiagent-based dispatching scheme for distributed generators for voltage support on distribution feeders," *IEEE Trans. Power Syst.*, vol. 22, no. 1, pp. 52–59, Feb. 2007.
- [8] L. B. Perera, G. Ledwich, and A. Ghosh, "Distribution feeder voltage support and power factor control by distributed multiple inverters," in *Proc. IEEE Elect. Power Energy Conf. (EPEC)*, Winnipeg, MB, Canada, Oct. 2011, pp. 116–121.
- [9] T. Niknam, A. Ranjbar, and A. Shirani, "Impact of distributed generation on Volt/Var control in distribution networks," in *Proc. IEEE Bologna Power Tech Conf.*, vol. 3, Bologna, Italy, Jun. 2003, pp. 7–14.
- [10] P. Hrisheeksha and J. Sharma, "Evolutionary algorithm based optimal control distribution system dispersed generation," *Int. J. Comput. Appl.*, vol. 14, pp. 31–37, Feb. 2010.
- [11] J. Olamaie and T. Niknam, "Daily Volt/Var control in distribution networks with regard to DGs: A comparison of evolutionary methods," in *Proc. IEEE Power India Conf.*, New Delhi, India, 2006, p. 6.
- [12] *Emulab—Network Emulation Testbed Home*. [Online]. Available: <http://www.emulab.net>
- [13] B. White *et al.*, "An integrated experimental environment for distributed systems and networks," in *Proc. 5th Symp. Oper. Syst. Design Implement.*, Boston, MA, USA, Dec. 2002, pp. 255–270.
- [14] *IEEE Standard for Synchrophasor Measurements for Power Systems*, IEEE Standard C37.118.2011-1, Dec. 28, 2011.
- [15] *IEEE Standard for Synchrophasor Data Transfer for Power Systems*, IEEE Standard C37.118.2011-2, Dec. 28, 2011.
- [16] *Networks and Communication Systems Branch: EMANE*. [Online]. Available: <http://cs.itd.nrl.navy.mil/work/emane/index.php>
- [17] *IEEE 802.11 Standard Working Group, Standard for Information Technology—Telecommunications and Information Exchange Between Systems—LAN/MAN Specific Requirements Part 11: Wireless LAN Medium Access Control (MAC) and Physical Layer (PHY) Specifications*, ANSI/IEEE Standard 802.11, 1999.
- [18] *IEEE Guide for Phasor Data Concentrator Requirements for Power System Protection, Control, and Monitoring*, IEEE Standard C37.244, May 10, 2013.
- [19] K. E. Martin, "Synchrophasor standards development—IEEE C37.118 & IEC 61850," in *Proc. 44th Hawaii Int. Conf. Syst. Sci.*, Kauai, HI, USA, Jan. 2011, pp. 1–8.
- [20] P. Nitesh and K. Khandeparkar, "Design and implementation of IEEE C37.118 based phasor data concentrator & PMU simulator for wide area measurement system," *Indian Inst. Technol.*, Mumbai, India, May. 2012.
- [21] F. Bidaud, *Simulation Solution: Power Factor Calculation by the Finite Element Method*, CEDRAT News, Meylan, France, Oct. 2011.
- [22] D. Shmilovitz, "On the definition of total harmonic distortion and its effect on measurement interpretation," *IEEE Trans. Power Del.*, vol. 20, no. 1, pp. 526–528, Jan. 2005.
- [23] W. M. Grady and R. J. Gilleskie, "Harmonics and how they relate to power factor," in *Proc. EPRI Power Qual. Issues Opportun. Conf. (PQA)*, San Diego, CA, USA, Nov. 1993, pp. 1–8.
- [24] A. G. Phadke, J. S. Thorp, and M. G. Adamiak, "A new measurement technique for tracking voltage phasors, local system frequency, and rate of change of frequency," *IEEE Trans. Power App. Syst.*, vol. PAS-102, no. 5, pp. 1025–1038, May 1983.
- [25] H. Gharavi, "Multichannel mobile ad hoc links for multimedia communications," *Proc. IEEE*, vol. 96, no. 1, pp. 77–96, Jan. 2008.
- [26] H. Gharavi and B. Hu, "Multigate communication network for smart grid," *Proc. IEEE*, vol. 99, no. 6, pp. 1028–1045, Jun. 2011.
- [27] P. Carvalho, P. F. Correia, and L. Ferreira, "Distributed reactive power generation control for voltage rise mitigation in distribution networks," *IEEE Trans. Power Syst.*, vol. 23, no. 2, pp. 766–772, May 2008.
- [28] H. Gharavi and C. Xu, "Traffic scheduling technique for smart grid advanced metering applications," *IEEE Trans. Commun.*, vol. 60, no. 6, pp. 1646–1658, Jun. 2012.
- [29] *IEEE 802.11s Task Group, Draft Amendment to Standard for Information Technology—Telecommunications and Information Exchange Between Systems—LAN/MAN Specific Requirements—Part 11: Wireless Medium Access Control (MAC) and Physical Layer (PHY) Specifications: Amendment: ESS Mesh Networking*, IEEE Standard P802.11s/D1.0, Nov. 2006.
- [30] P. Jacquet, P. Muhlethaler, and A. Qayyum, "Optimized link state routing protocol," in *IETF MANET: Internet Draft*, Nov. 1998.
- [31] T. H. Chen *et al.*, "Feasibility study of upgrading primary feeders from radial and open-loop to normally closed-loop arrangement," *IEEE Trans. Power Syst.*, vol. 19, no. 3, pp. 1308–1316, Aug. 2004.
- [32] W. T. Huang, T. H. Chen, G. C. Pu, Y. F. Hsu, and T. Y. Guo, "Assessment of upgrading existing primary feeders from radial to normally closed loop arrangement," in *Proc. IEEE Power Eng. Soc. Transmiss. Distrib. Conf.*, vol. 3, Yokohama, Japan, 2002, pp. 2123–2128.
- [33] *Ubuntu: The Leading OS for PC, Tablet, Phone and Cloud*. [Online]. Available: <http://www.ubuntu.com>



**Hamid Gharavi** (M'79–SM'90–F'92–LF'13) received the Ph.D. degree from Loughborough University, Loughborough, U.K., in 1980.

He joined the Visual Communication Research Department, AT&T Bell Laboratories, Holmdel, NJ, USA, in 1982. He was then transferred to Bell Communications Research (Bellcore), Red Bank, NJ, after the AT&T-Bell divestiture, where he became a Consultant on video technology and a Distinguished Member of Research Staff. In 1993, he joined Loughborough University, as a Professor and Chair of Communication Engineering. Since September 1998, he has been with the National Institute of Standards and Technology (NIST), U.S. Department of Commerce, Gaithersburg, MD, USA. He was a core member of Study Group XV (Specialist Group on Coding for Visual Telephony) of the International Communications Standardization Body CCITT (ITU-T). His research interests include smart grid, wireless multimedia, mobile communications and wireless systems, mobile ad hoc networks, and visual communications. He holds eight U.S. patents and has over 100 publications related to these topics.

Dr. Gharavi received the Charles Babbage Premium Award from the Institute of Electronics and Radio Engineering in 1986, and the IEEE Circuits and Systems Society (CAS) Darlington Best Paper Award in 1989. He served as a Distinguished Lecturer of the IEEE Communication Society. In 1992, he was elected a Fellow of IEEE for his contributions to low-bit-rate video coding and research in sub-band coding for video applications. He has been a Guest Editor for a number of special issues, including *Smart Grid: The Electric Energy System of the Future*, PROCEEDINGS OF THE IEEE; *Sensor Networks and Applications*, PROCEEDINGS OF THE IEEE; and *Wireless Multimedia Communications*, PROCEEDINGS OF THE IEEE. He was a Technical Committee Program Co-Chair for IEEE SmartGridComm in 2010 and 2012. He served as a Member of the Editorial Board of PROCEEDINGS OF THE IEEE from January 2003 to December 2008. From January 2010 to December 2013, he served as Editor-in-Chief of the IEEE TRANSACTIONS ON CAS FOR VIDEO TECHNOLOGY. He is currently a member of the Editorial Boards of IEEE ACCESS, and is the new Editor-in-Chief of IEEE WIRELESS COMMUNICATIONS.

**Bin Hu** (SM'13), photograph and biography not available at the time of publication.